
Single origin of the nodal and antinodal gaps in cuprates

YVES NOAT^{1,*}, ALAIN MAUGER² and WILLIAM SACKS²

¹ *Institut des Nanosciences de Paris (INSP), UMR 7588,*

² *Institut de Minéralogie, de Physique des Matériaux, et de Cosmochimie (IMPMC), UMR 7590,*

*Sorbonne Universités,
4 place Jussieu, 75252 Paris Cedex 05, France*

* *Corresponding author: yves.noat@insp.jussieu.fr*

PACS 74.72.h – First pacs description
PACS 74.20.Mn – Second pacs description
PACS 74.20.Fg – Third pacs description

Abstract –Recent angle-resolved photoemission electron spectroscopy (ARPES) experiments demonstrate that the momentum dependence of the spectral gap in underdoped cuprates does not follow a pure d -wave form [H. Anzai et al., Nat. Comm. 4, 1815 (2013)]. This deviation is highly controversial. It has often been interpreted as a proof of the non-superconducting origin of the antinodal gap in the underdoped regime. In this article, we show that the measured angular dependence of the spectral gap can be explained by the basic nature of pairs in high- T_c cuprates. Hole pairs, or *pairons*, form as a result of the local antiferromagnetic environment on the scale ξ_{AF} , the magnetic coherence length. The spatial extension of the pairon wavefunction beyond first nearest neighbours gives rise to the anomalous angular dependence of the gap, in quantitative agreement with experiments. This simple interpretation strongly indicates a common origin of the nodal and antinodal gaps.

Introduction: Are there two energy scales in superconducting cuprates?

One of the most challenging problems of high- T_c cuprates is the interpretation of the spectral gap. Contrary to conventional superconductors where the spectral gap vanishes at the critical temperature, as described by the Bardeen-Cooper-Schrieffer (BCS) theory [1], in cuprates a gap persisting at the critical temperature T_c , the so-called pseudogap, is directly observed in angle resolved photoemission spectroscopy (ARPES) [2,3] or scanning tunneling spectroscopy [4]. Whether or not the pseudogap is linked to superconductivity remains a fundamental question.

More recently, low-temperature experiments revealed a non-trivial angular dependence of the gap as a function of doping. While in overdoped samples the gap follows a strictly d -wave behavior, a clear deviation from d -wave is observed on the underdoped side of the phase diagram

(see [5] and Refs. therein). This so called two-gap behavior was first revealed by electronic Raman scattering [6] and photoemission [7] and later confirmed by tunneling spectroscopy [8]. It is most often interpreted as the result of the competition between superconductivity and the phase responsible for the pseudogap [7,9–11].

As first noted by Kondo et al. [12] and Terashima et al. [13], the shape of $\Delta(\theta)$ can be properly described by including an additional harmonic term to the usual d -wave dependence:

$$\Delta(\theta) = \Delta_0 [B \cos(2\theta) + (1 - B) \cos(6\theta)] \quad (1)$$

An analogous formula was later used by Anzai et al. [14] who carefully studied the angular dependence of the gap as a function of doping. The fit of the ARPES data can be used to determine the doping dependence of the nodal and antinodal gaps. By this procedure, Anzai et al. found a dome shape for the nodal gap, which was then interpreted as the order parameter [14], suggesting that the super-

conding (SC) state is restricted to the near nodal region in k -space (i.e. in the Fermi arc region, as in Ref. [10]).

A separate analysis performed by Vishik et al. [11] led to a completely different conclusion, namely that the nodal gap is almost doping independent in the underdoped regime while it is almost equal to the antinodal value in the overdoped regime. The crossover between the two behaviors occurs for a doping value $p \sim 0.18$ (i.e. slightly higher than the optimum doping value $p \sim 0.16$). This discrepancy between the two analyses clearly indicates that a more careful attention should be paid to the method used to infer the nodal gap value. From an overview of the literature on this question [5], one concludes that the connection of the nodal and antinodal gaps to the SC state remains an important unsolved issue for understanding high- T_c superconductivity.

In this paper, we reconcile the contradictory experimental analysis and give a simple explanation for the angular dependence of the gap in the whole doping range, from underdoped to overdoped regimes. Our analysis demonstrates that the latter is essentially governed by the doping dependence of the antiferromagnetic coherence length ξ_{AF} , which determines the size of pairs forming the SC condensate.

Angular dependence of the gap

There is an overall agreement that, at least in the overdoped regime, the spectral gap as a function of angle has a simple d -wave form:

$$\Delta(\vec{k}) = \Delta_p [\cos(k_x a) - \cos(k_y a)] \quad (2)$$

At the Fermi surface ($k = k_F$), this formula can be well approximated by

$$\Delta(\theta) \simeq \Delta_p \cos(2\theta) \quad (3)$$

The angle in the above formula is taken from the (π, π) corner of the first Brillouin zone. With these coordinates, the antinodal direction $(\pi, 0)$ corresponds to $\theta = 0$ while the nodal direction ($k_x = k_y$) corresponds to $\theta = \frac{\pi}{4}$.

Deviations from this standard form have been observed in the underdoped regime by several groups [11–15]. Such deviations, as in Fig. 1 and 2, occur if the doping is lower than some value, which varies from experiment to experiment (see [5] for a review). The latter is generally higher than the optimum doping value [5].

Although the angular dependence of $\Delta(\theta)$ includes new harmonics as mentioned above, in the underdoped regime the overall shape still has a d -wave character. We find it useful to reformulate Eq. 1, in an alternate algebraic form:

$$\Delta(\theta) = \Delta_p [1 - \alpha \sin^2(2\theta)] \cos(2\theta) \quad (4)$$

In this form, the gap at the antinode is by definition $\Delta(\theta = 0) = \Delta_p$ while the so-called nodal gap is defined by:

$$\Delta_N = -\frac{1}{2} \frac{d\Delta(\theta)}{d\theta} \Big|_{\theta=\frac{\pi}{4}} = \Delta_p (1 - \alpha). \quad (5)$$

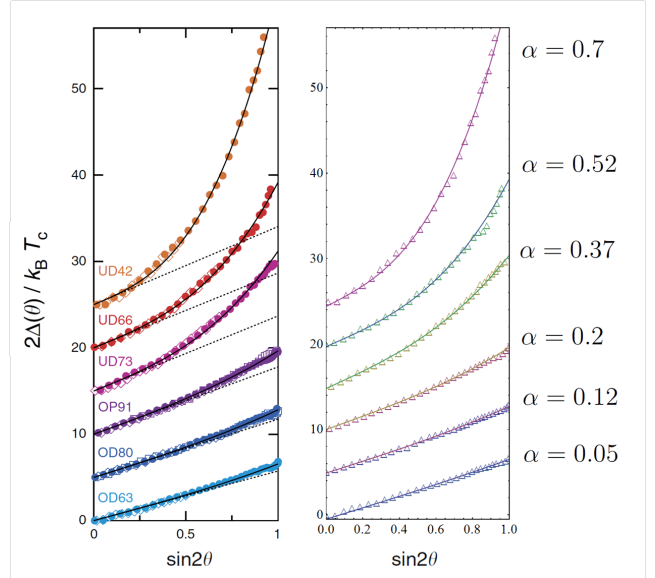


Fig. 1: (Color online) Left panel: Gap as a function of $\sin(\theta)$ from the work of Anzai et al. [14]; Right panel: Fit of the data $\Delta(\theta)$ using formula 4. The values of α deduced from the fits are indicated on the right side for each doping value. (Note that in ref. [14] the angle is measured from the node.)

Note that while the common name often given to Δ_N is the nodal ‘gap’, it is in fact *the slope* of $\Delta(\theta)$ at the node. Thus, α appears as the key parameter giving rise to the difference between the nodal and the antinodal gaps.

We have fit the experimental spectra from Anzai et al. [14] for different doping values. As shown in Fig. 1 the agreement between Eq.4 and the experiment is remarkable. While in the overdoped regime, the shape of $\Delta(\theta)$ is perfectly d -wave, a clear deviation is observed in the underdoped side of the phase diagram. This deviation grows as the doping is lowered. We have also analysed data from Vishik et al. [11] as well as the one reported by Hashimoto et al. [15]. As shown in Fig. 2, Eq. 4 also perfectly reproduces the angular dependence of the gap they have observed in a wide doping range.

We now come to the determination of the slope of $\Delta(\theta)$, i.e. the nodal gap. In ref. [11], the latter was derived from the linear fit of the gap value near the node. This method, however, is not correct, because the curvature of the experimental curve does not vanish at any value of θ in the underdoped regime, so that the slope found by assuming *a priori* a linear behavior near the node depends on both the number of experimental points and the extension in θ chosen to make such a fit.

Contrary to the procedure used in [11], where the slope was tentatively estimated from the experimental points near the node, we calculate the nodal gap from the fit of $\Delta(\theta)$ using Eq. 5. This is a fundamental point in the analysis. Indeed, it should be stressed that in order to deduce precisely the slope of $\Delta(\theta)$ at the node, given by Eq. 4, one needs to properly fit the whole curve from

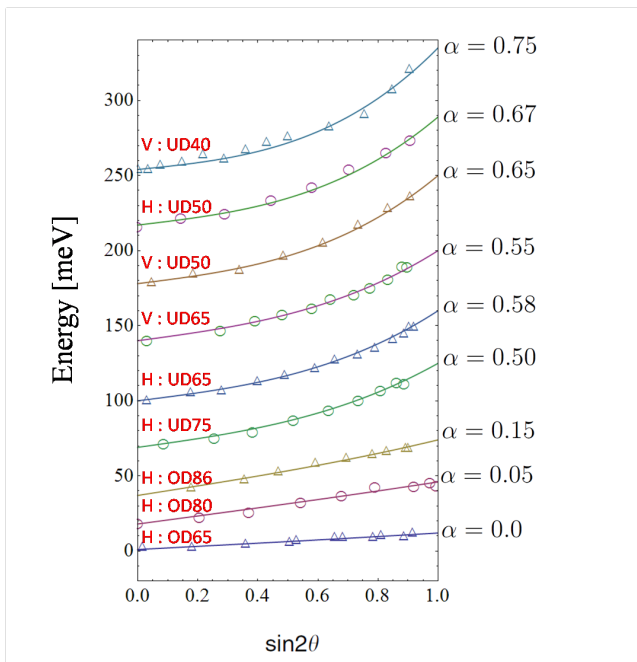


Fig. 2: (Color online) Angular dependence of the gap from Vishik et al. [11] (spectra labeled with letter ‘V’) and Hashimoto et al. [15] (spectra labeled with letter ‘H’); Right panel: Fit of $\Delta(\theta)$ with formula 4. The values of α deduced from the fits are indicated on the right side for each doping value.

the node to the antinode. This difference explains the discrepancy in the determination of Δ_N reported in [11] and [14].

The nodal gap inferred from our analysis is plotted in Fig. 3 which proves the consistency of the data of both Refs. [14] and [11]. Although the nodal gap has a dome shape, it is nevertheless clear that it does not follow T_c . The maximum of $\Delta_N(p)$ is shifted with respect to that of $T_c(p)$. Moreover $\Delta_N(p)$ does not vanish for $p = p_{im}$ where the superconducting phase first appears. This finding seems to discard the hypothesis that the nodal gap is directly the order parameter, contrary to the conclusion raised in [14].

In addition, the doping dependence of the parameter α which characterizes the deviation from d -wave, closely follows the one deduced from the data of Anzai et al. [14], which gives good confidence in our analysis.

The present approach thus reconciles ARPES experiments where contradictory interpretations were given. We now turn to the physical origin of the anomalous angular dependence.

Pairons: hole pairs in a short-range antiferromagnetic background

As demonstrated by pioneering works in the early nineties in the context of the Hubbard or $t - J$ hamiltonians, two holes in an antiferromagnetic background can form a bound state for a sufficiently large t/J ratio [16–19],

with the expected d -wave symmetry [20]. These works strongly suggest the existence of hole pairs in an AF background, although the description in terms of strongly correlated electrons might fail in the overdoped side of the phase diagram [21].

We have extended this concept to realistic systems [22] where the key point is the small but finite antiferromagnetic coherence length. Indeed, in cuprates, the long range antiferromagnetic state is broken by hole doping at $p = p_{AF}$, giving rise to a superconducting state with short-range AF correlations for $p > p_{im}$ [23]. The superconducting phase emerges from the metallic phase in the doping range $p_{im} < p < p_{m}$.

In recent articles, we have proposed that high- T_c superconductivity can be explained in terms of the formation of hole pairs, or *pairons*, in their local antiferromagnetic environment [22], on the scale of ξ_{AF} . In [22] each pairon is associated with an AF cell of area ξ_{AF}^2 which naturally explains the linear behavior of the antinodal gap energy with doping.

Two different temperatures can be distinguished corresponding respectively to the formation of the pairs and their condensation, both being linked to a single energy scale, J , the exchange energy. Pairons form at a temperature T^* higher than the critical temperature and undergo a Bose-like condensation at T_c as a result of repulsive pair-pair interactions [24].

The pairon model is supported by several experimental facts, in particular by

- (i) the presence of a low-temperature energy gap within the vortex core where coherence is lost [25], which strongly suggests the presence of preformed pairs,
- ii) the concomitant disappearance of superconductivity and antiferromagnetic correlations as a function of doping (for $p = p_{m}$) [26],
- iii) the scaling of the critical temperature with the exchange energy $T_c \propto J$ [27], which is a direct consequence of the nature of pairons and of the corresponding phase diagram [22].

The nature of pairons is revealed in the excitation spectrum as a function of temperature. Indeed, two well-defined signatures are observed in ARPES measurements: a Fermi arc near the node at T_c and below [28] and a gap without coherence peaks, the pseudogap, in the antinode above T_c [2, 3]. The latter display the characteristic Bogoliubov quasiparticle dispersion indicating preformed pairs [29, 30]. In the pairon model, the Fermi arc is the result of fermion excitations, due to the composite fermion character of pairons, while the pseudogap is a manifestation of an incoherent state of excited pairons, absent in a conventional BCS superconductor [31].

Origin of the angular dependence of the gap

The pairon model also provides a physical explanation for the observed gap angular dependence. Indeed, to understand the shape of $\Delta(\theta)$, one needs to consider how

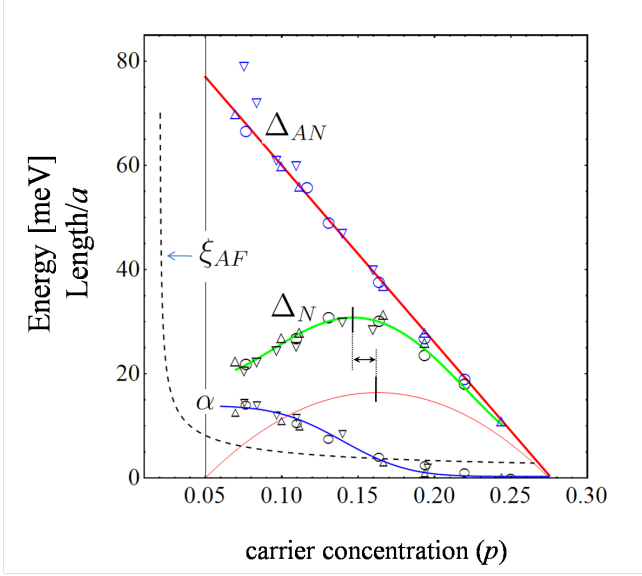


Fig. 3: (color online) Phase diagram deduced from the fits from experimental data taken from Anzai et al. [14] (circles), Vishik et al. [11] (inverted triangles) and Hashimoto et al. [15] (triangles). The nodal and antinodal gaps and the parameter α deduced from the fits as a function of doping.

the gap is modified at low doping as the size of antiferromagnetic correlations increases. For this purpose, we start from the expression of the hole pair wavefunction in relative coordinates. In our previous work [31], only first nearest neighbours were considered (red dots in Fig. 4):

$$\begin{aligned} \psi_{\mathbf{p}}^{(1)}(\vec{r}) = & \frac{1}{\sqrt{4}} [\varphi(\vec{r} - a\hat{x}) + \varphi(\vec{r} + a\hat{x})] \\ & - [\varphi(\vec{r} - a\hat{y}) - \varphi(\vec{r} + a\hat{y})] \end{aligned} \quad (6)$$

where a is the lattice parameter, and $\varphi(\vec{r}) = e^{-\frac{r^2}{2b^2}} / \sqrt{2\pi b^2}$. The parameter b fixes the spatial extension of the pair wavefunction in relative coordinates. The overlap between the various amplitudes in Eq. 6 has been neglected. Note that the sign in the above formula originates from the antiferromagnetic symmetry which imposes that the wavefunction must vanish in the lattice diagonal (corresponding to the nodal direction in k -space).

It follows that the associated gap is expressed in the standard d -wave form (Eq. 2) [31]:

$$\Delta(k) = \tilde{\varphi}(k_F) A_1 g_1(k_x, k_y), \quad (7)$$

where $\tilde{\varphi}(k_F)$ is the Fourier transform of $\varphi(\vec{r})$ taken at $k = k_F$, A_1 is a constant and

$$g_1(k_x, k_y) = \cos(k_x a) - \cos(k_y a) \quad (8)$$

As the doping is lowered, the size of the pairons, of the order of ξ_{AF} , increases. The delocalized wavefunction must then include the contribution of next nearest neighbours (blue dots in Fig. 4):

$$\psi_{\mathbf{p}}(\vec{r}) = \sum_i \psi_{\mathbf{p}}^{(i)}(\vec{r}) \quad (9)$$

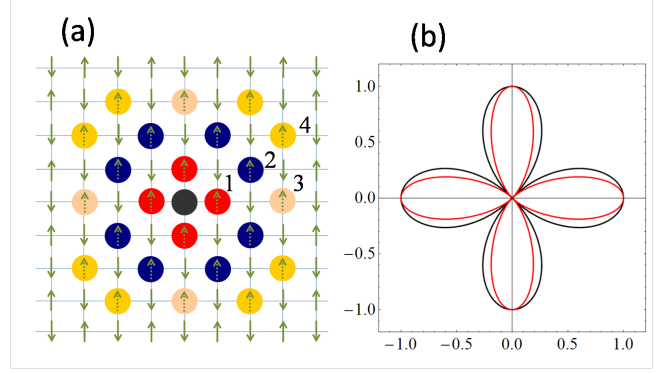


Fig. 4: (color online) a) Illustration of a hole pair in its antiferromagnetic environment. The red/blue/pink/yellow dots correspond respectively to first, second, third and fourth nearest neighbours for the hole pairs, one hole (black hole) being located in the center. b) Pure d -wave order parameter ($\alpha = 0$, black curve), compared to gap including higher harmonics term ($\alpha = 0.7$, red curve). As can be noted, the gap is reduced near the node compared to the pure d -wave gap (black curve).

with $\psi_{\mathbf{p}}^{(i)}(\vec{r}) \propto \sum_{\mathbf{r}_j} c_j \varphi(\vec{r} - \vec{r}_j)$; the sum runs over all the i^{th} nearest neighbours and $c_j = \pm 1$ determines the sign of each term and is imposed by the AF symmetry, as explained below. The second neighbour correction is expressed as

$$\begin{aligned} \psi_{\mathbf{p}}^{(2)}(\vec{r}) \propto & [\varphi(\vec{r} - 2a\hat{x} - 2a\hat{y}) + \varphi(\vec{r} - a\hat{x} - 2a\hat{y})] \\ & + \varphi(\vec{r} + a\hat{x} - 2a\hat{y}) - \varphi(\vec{r} + 2a\hat{x} - a\hat{y}) \\ & - \varphi(\vec{r} + 2a\hat{x} + a\hat{y}) + \varphi(\vec{r} + a\hat{x} + 2a\hat{y}) \\ & + \varphi(\vec{r} - a\hat{x} + 2a\hat{y}) - \varphi(\vec{r} - 2a\hat{x} + a\hat{y}) \end{aligned} \quad (10)$$

The Fourier transform of the wavefunction $\psi_{\mathbf{p}}(\vec{r})$ (Eq. 9) then gives rise to additional terms. As described in a previous article [31], the pairon wavefunction can then be expressed as a superposition of Cooper pairs in k -space. Extending the calculation derived in [31], we obtain the gap function:

$$\Delta(\vec{k}) = \tilde{\varphi}(k_F) \sum_i A_i g_i(k_x, k_y) \quad (11)$$

where $\tilde{\varphi}(k_F) A_i g_i(k_x, k_y)$ is the contribution to the gap amplitude of the i^{th} nearest neighbours. The first term has the standard d -wave form, while the second nearest neighbour contribution, deduced from Eq. 10, is expressed as:

$$\begin{aligned} g_2(\vec{k}) = & [-\cos(2k_x a + k_y a) + \cos(k_x a + 2k_y a)] \\ & + [\cos(k_x a - 2k_y a) - \cos(2k_x a - k_y a)] \end{aligned} \quad (12)$$

There are two possible signs for the second neighbour correction to the wavefunction, $g_2(\vec{k})$. The positive sign in front of the bracket was chosen in order to properly describe the experimental results. It is compatible with the

AF symmetry, introducing new nodal lines in the second neighbour correction, in agreement with the higher angular harmonics of Eq.4. This effect *reduces* the nodal gap compared to the antinodal value (see Fig. 4b).

Discussion

The previous expression accounts quantitatively for the angular dependence of the gap. The reason is that, for any choice of A_1 and A_2 , the above formula is strictly equivalent to formula 4 used for the fits (i.e. there is an equivalence between the parameter α used in Eq. 4 and A_2/A_1). The correspondence between the parameter using formula 4 and 11 restricted to second neighbours can be found in table 1. It is relatively straightforward to express the coefficients A_i reflecting the weight of the i^{th} neighbour in the hole pair wavefunction. We have numerically evaluated A_i for $i = 3$ and 4 which turn out to be negligible so that only second neighbours contribute to the angular dependence of the gap at low doping.

The second neighbour correction to the gap must be directly related to the extension of the pairon wavefunction, i.e. to the size of the AF correlations. Let us rewrite Eq. 11 in the equivalent form:

$$\Delta(\vec{k}) = \tilde{\varphi}(k_F) A_1 \left[g_1(k_x, k_y) + \frac{A_2}{A_1} g_2(k_x, k_y) \right] \quad (13)$$

Assuming that $\frac{A_2}{A_1} = \eta e^{-\frac{d_2-d_1}{\xi_{AF}}}$, with $d_1 = a$ and $d_2 = \sqrt{5}a$ being the distance between two holes when first and second neighbours sites are occupied (red and blue dots in Fig. 4), for each doping value, the correction to pure d -wave symmetry can be found.

The doping dependence of the antiferromagnetic correlation length has been deduced from neutron experiments and is close to $1/\sqrt{p}$ [32,33]. We take

$$\xi_{AF}(p) \propto \frac{a}{\sqrt{p - p_{AF}}}, \quad (14)$$

where a is the lattice parameter. The parameter p_{AF} has been introduced in order to describe more precisely the data of Ref. [33] than with the $1/\sqrt{p}$ dependence. It accounts for the divergence due to the long-range order onset at the AF transition for $p = p_{AF} \approx 0.02$. The values of η corresponding to each doping value is given in table 1.

As indicated in the table, $\xi_{AF}(p)$ varies between $\sim 3a$, and $\sim 6a$ in the entire SC doping range. Since $a \sim 3.8 \text{ \AA}$, it explains why the third and fourth nearest neighbours do not have a significant contribution. This leaves only the second neighbour contribution (with the coefficient A_2) to fit the experimental curves of $\Delta(\theta)$. The precise fits to the experimental ARPES data can be done with either using the α parameter, and Eq.4, or the ratio A_2/A_1 , using Eq.13.

Both the α parameter and the ratio A_2/A_1 , representing the extension of the pairon wavefunction to the second neighbors, vary continuously and monotonically with doping which is a strong indication that Δ_N and Δ_{AN} have

a single origin. The evolution of the shape of $\Delta(\theta)$ as a function of doping can thus be coherently interpreted as a direct consequence of the spatial extension of pairons, which follows $\xi_{AF}(p)$ as a function of hole concentration as predicted in [22]. However it should be stressed that another microscopic model, such as resonant valence bond theory [34], which would predict a wavefunction with a similar symmetry cannot be completely ruled out.

As shown in the phase diagram of Fig. 3, the nodal gap has a dome shape but does not follow T_c . As mentioned before, this behavior demonstrates that the nodal gap is not the order parameter. Examining its shape, it is tempting to extrapolate the behavior of Δ_N for lower doping values. Its finite value at $p = p_m$ would suggest that a non-zero nodal gap persists in the small doping range $p_{AF} < p < p_m$ between the long range AF order Mott transition and the superconducting state where the sample is in an insulating state with short-range AF correlations [23].

This hypothesis is in agreement with the findings of Chatterjee et al. [35] who measured the ARPES spectra for a strongly underdoped non-superconducting sample of $\text{Bi}_2\text{Sr}_2\text{CaCu}_2\text{O}_{8+\delta}$ ($p \approx 0.04$), and found a gap with nodes, as in the SC state. While the absence of deviation from d -wave symmetry in this sample is not completely understood, the presence of a gap suggests the existence of non-condensed pairons in this system. Compatible with this discussion is the recent discovery of a gap with a similar angular dependence as in cuprates in electron-doped Mott insulator Sr_2IrO_4 [36,37]. In both cases, it is remarkable that the presence of a gap without superconducting coherence may reveal an incoherent gas of pairons in the insulating phase.

Conclusion

In this article, we have shown that the deviation of the superconducting gap from pure d -wave symmetry observed in cuprates by ARPES can be interpreted as the result of the existence of hole pairs, or *pairons*, in their local antiferromagnetic background. In the overdoped regime, the gap has a pure d -wave symmetry, due to the small extension of the pairon wavefunction, restricted to first nearest neighbours. In the underdoped regime, the pairon wavefunction extends beyond first nearest neighbours, on the scale of the antiferromagnetic coherence length, which reduces the gap amplitude near the nodal direction.

The model reproduces quantitatively the measured angular dependence of the gap and its doping dependence. Furthermore it reconciles some divergences in the interpretation of ARPES data in the literature. One concludes that the nodal and antinodal gaps originate from the same phenomenon, both intimately linked to the superconducting phase transition.

p	T_c (K)	$\frac{2\Delta}{k_B T_c}$	Δ_p (meV)	Δ_N (meV)	α	η	$\frac{A_2}{A_1}$	ξ_{AF} (a units)
0.25	37.5	5.6	9	9	0	0	0	2.9
0.22	63	7	19	19	0.05	0.015	0.01	3.16
0.194	80	7.8	26.9	23.6	0.12	0.051	0.036	3.4
0.164	91	9.6	37.7	30.16	0.2	0.082	0.06	3.7
0.131	73	15.6	49	30.87	0.37	0.185	0.13	4.2
0.117	66	19.6	55.8	26.8	0.52	0.275	0.2	4.5
0.077	42	36.8	66.6	21.9	0.7	0.364	0.295	5.9

Table 1: Experimental parameters (T_c , Δ_p) from Anzai et al [14] and parameters deduced from the fits (the nodal gap Δ_N , α , η , $\frac{A_2}{A_1}$) as a function of the doping value p . We also indicate the calculated value of $\xi_{AF}(p)$ (a units) obtained using Eq. 14 with $p_{AF} = 0.02$ for each doping value.

REFERENCES

- [1] J. Bardeen, L. Cooper, J. Schrieffer, Theory of Superconductivity, Phys. Rev. **108** 1175 (1957).
- [2] H. Ding, T. Yokoya, J. C. Campuzano, T. Takahashi, M. Randeria, M. R. Norman, T. Mochiku, K. Kadowaki and J. Giapintzakis, Spectroscopic evidence for a pseudogap in the normal state of underdoped high- T_c superconductors, Nature **382**, 5154 (1996).
- [3] A.G. Loeser, Z. Shen, D.S. Dessau, D.S. Marshall, C.H. Park, P. Fournier, A. Kapitulnik, Excitation Gap in the Normal State of Underdoped $\text{Bi}_2\text{Sr}_2\text{CaCu}_2\text{O}_{8+\delta}$, Science **273**,325 (1996).
- [4] Ch. Renner, B. Revaz, J.-Y. Genoud, K. Kadowaki, and Ø. Fischer, Pseudogap precursor of the superconducting gap in under- and overdoped $\text{Bi}_2\text{Sr}_2\text{CaCu}_2\text{O}_{8+\delta}$, Phys. Rev. Lett., **80** 149 (1998).
- [5] Tepei Yoshida, M. Hashimoto, I. M. Vishik, Z.-X. Shen, and A. Fujimori, Pseudogap, Superconducting Gap, and Fermi Arc in High- T_c Cuprates Revealed by Angle-Resolved Photoemission Spectroscopy, J. Phys. Soc. Jpn. **81**, 011006 (2012).
- [6] M. Le Tacon, A. Sacuto, A. Georges, G. Kotliar, Y. Gallais, D. Colson and A. Forget, Two energy scales and two distinct quasiparticle dynamics in the superconducting state of underdoped cuprates, Nat. Phys. **2**, 537543 (2006).
- [7] Kiyohisa Tanaka, W. S. Lee, D. H. Lu, A. Fujimori, T. Fujii, Risdiana, I. Terasaki, D. J. Scalapino, T. P. Devereaux, Z. Hussain, Z.-X. Shen, Distinct Fermi-Momentum-Dependent Energy Gaps in Deeply Underdoped $\text{Bi}2212$, **314**, 1910-1913 (2006).
- [8] A. Pushp, C. V. Parker, A. N. Pasupathy, K. K. Gomes, S. Ono, J. Wen, Z. Xu, G. Gu, and A. Yazdani, Extending Universal Nodal Excitations Optimizes Superconductivity in $\text{Bi}_2\text{Sr}_2\text{Ca}_2\text{CuO}_{8+\delta}$, Science **324**, 1689-1693 (2009).
- [9] Takeshi Kondo, R. Khasanov, T. Takeuchi, J. Schmalian and A. Kaminski, Competition between the pseudogap and superconductivity in the high- T_c copper oxides, Nature **457**, 296300 (2009).
- [10] T. Yoshida, M. Hashimoto, S. Ideta, A. Fujimori, K. Tanaka, N. Mannella, Z. Hussain, Z.-X. Shen, M. Kubota, K. Ono, Seiki Komiya, Yoichi Ando, H. Eisaki, and S. Uchida, Universal versus Material-Dependent Two-Gap Behaviors of the High- T_c Cuprate Superconductors: Angle-Resolved Photoemission Study of $\text{La}_{2-x}\text{Sr}_x\text{CuO}_4$, Phys. Rev. Lett. **103**, 037004 (2009).
- [11] I. M. Vishik, M. Hashimoto, Rui-Hua He, Wei-Sheng Lee, Felix Schmitt, Donghui Lu, R. G. Moore, C. Zhang, W. Meevasana, T. Sasagawa, S. Uchida, Kazuhiro Fujita, S. Ishida, M. Ishikado, Yoshiyuki Yoshida, Hiroshi Eisaki, Zahid Hussain, Thomas P. Devereaux, and Zhi-Xun Shen, Phase competition in trisected superconducting dome, PNAS **109**, 18332-18337 (2012).
- [12] Takeshi Kondo, T. Takeuchi, A. Kaminski, S. Tsuda, and S. Shin, Evidence for Two Energy Scales in the Superconducting State of Optimally Doped $(\text{Bi,Pb})_2(\text{Sr,L a})_2\text{CuO}_{6+\delta}$, Phys. Rev. Lett. **98**, 267004 (2007).
- [13] K. Terashima, H. Matsui, T. Sato, T. Takahashi, M. Kofu, and K. Hirota, Anomalous Momentum Dependence of the Superconducting Coherence Peak and Its Relation to the Pseudogap of $\text{La}_{1.85}\text{Sr}_{0.15}\text{CuO}_4$, Phys. Rev. Lett. **99**, 017003 (2007).
- [14] H. Anzai, A. Ino, M. Arita, H. Namatame, M. Taniguchi, M. Ishikado, K. Fujita, S. Ishida and S. Uchida, Relation between the nodal and antinodal gap and critical temperature in superconducting $\text{Bi}2212$, Nature Communications **4**, 1815 (2013).
- [15] Makoto Hashimoto, Inna M. Vishik, Rui-Hua He, Thomas P. Devereaux and Zhi-Xun Shen, Energy gaps in high-transition-temperature cuprate superconductors, Nature Physics, **10**, p 483 (2014).
- [16] Efthimios Kaxiras and Efstratios Manousakis, Hole dynamics in the two-dimensional strong-coupling Hubbard Hamiltonian, Phys. Rev. B **38**, 866(R) (1988).
- [17] J. A. Riera and A. P. Young, Binding of holes in one-band models of oxide superconductors, Phys. Rev. B **39**, 9697(R) (1989).
- [18] J. Bonca, P. Prelovek, and I. Sega, Exact-diagonalization study of the effective model for holes in the planar antiferromagnet, Phys. Rev. B **39**, 7074 (1989).
- [19] Y. Hasegawa and D. Poilblanc, Hole dynamics in the t-J model: An exact diagonalization study, Phys. Rev. B **40**, 9035 (1989).
- [20] Didier Poilblanc, José Riera and Elbio Dagotto, d-wave bound state of holes in an antiferromagnet, Phys. Rev. B **49**, 12318 (1994).
- [21] D. C. Peets, D. G. Hawthorn, K. M. Shen, Young-June Kim, D. S. Ellis, H. Zhang, Seiki Komiya, Yoichi Ando, G. A. Sawatzky, Ruixing Liang, D. A. Bonn, and W. N. Hardy, X-Ray Absorption Spectra Reveal the Inapplica-

- bility of the Single-Band Hubbard Model to Overdoped Cuprate Superconductors, *Phys. Rev. Lett.* **103**, 087402 (2009).
- [22] William Sacks, Alain Mauger and Yves Noat, Cooper pairs without glue in high-Tc superconductors: A universal phase diagram, *Euro. Phys. Lett* **119**, 17001 (2017).
- [23] H. Takagi, T. Ido, S. Ishibashi, M. Uota, S. Uchida, and Y. Tokura, Superconductor-to-nonsuperconductor transition in $(\text{La}_{1-x}\text{Sr}_x)_2\text{CuO}_4$ as investigated by transport and magnetic measurements, *Phys. Rev. B* **40**, 2254 (1989).
- [24] William Sacks, A. Mauger, Y. Noat, Pair-pair interactions as a mechanism for high-Tc superconductivity, *Superconduct. Sci. Technol.*, **28** 105014 (2015).
- [25] Ch. Renner, B. Revaz, K. Kadowaki, I. Maggio-Aprile and Ø. Fischer, Observation of the Low Temperature Pseudogap in the Vortex Cores of $\text{Bi}_2\text{Sr}_2\text{CaCu}_2\text{O}_{8+\delta}$, *Phys. Rev. Lett.* **80**, 3606 (1998).
- [26] R. Yoshizaki, N. Ishikawa, H. Sawada, E. Kita, A. Tasaki, Magnetic susceptibility of normal state and superconductivity of $\text{La}_{2-x}\text{Sr}_x\text{CuO}_4$, *Physica C* **166**, 417-422 (1990).
- [27] Rinat Ofer, Galina Bazalitsky, Amit Kanigel, Amit Keren, Assa Auerbach, James S. Lord, and Alex Amato, Magnetic analog of the isotope effect in cuprates, *Phys. Rev. B* **74**, 220508(R) (2006).
- [28] M. R. Norman, H. Ding, M. Randeria, J. C. Campuzano, T. Yokoya, T. Takeuchi, T. Takahashi, T. Mochiku, K. Kadowaki, P. Guptasarma and D. G. Hinks, Destruction of the Fermi surface in underdoped high-Tc superconductors, *Nature* **392**, 157160 (1998).
- [29] A. Kanigel, U. Chatterjee, M. Randeria, M. R. Norman, G. Koren, K. Kadowaki, and J. C. Campuzano, Evidence for Pairing above the Transition Temperature of Cuprate Superconductors from the Electronic Dispersion in the Pseudogap Phase, *Phys. Rev. Lett.* **101**, 137002 (2008).
- [30] M. Shi, A. Bendounan, E. Razzoli, S. Rosenkranz, M. R. Norman, J. C. Campuzano, J. Chang, M. Månsson, Y. Sassa, T. Claesson, Spectroscopic evidence for preformed Cooper pairs in the pseudogap phase of cuprates, *EPL* **88**, 27008 (2009).
- [31] William Sacks, A. Mauger and Y. Noat, Origin of the Fermi arcs in cuprates: a dual role of quasiparticle and pair excitations, *Journal of Physics: Condensed Matter*, **30**, 475703 (2018).
- [32] R. J. Birgeneau, D. R. Gabbe, H. P. Jenssen, M. A. Kastner, P. J. Picone, T. R. Thurston, G. Shirane, Y. Endoh, M. Sato, K. Yamada, Y. Hidaka, M. Oda, Y. Enomoto, M. Suzuki, and T. Murakami, Antiferromagnetic spin correlations in insulating, metallic, and superconducting $\text{La}_{2-x}\text{Sr}_x\text{CuO}_4$, *Phys. Rev. B* **38**, 6614 (1988);
- [33] T. R. Thurston, R. J. Birgeneau, M. A. Kastner, N. W. Preyer, G. Shirane, Y. Fujii, K. Yamada, Y. Endoh, K. Kakurai, M. Matsuda, Y. Hidaka, and T. Murakami, Neutron scattering study of the magnetic excitations in metallic and superconducting $\text{La}_{2-x}\text{Sr}_x\text{CuO}_{4-y}$, *Phys. Rev. B* **40**, 4585 (1989).
- [34] P.W. Anderson, The Resonating Valence Bond State in La_2CuO_4 and Superconductivity, *Science* **235**, 1196-1198 (1987).
- [35] U. Chatterjee, M. Shi, D. Ai, J. Zhao, A. Kanigel, S. Rosenkranz, H. Raffy, Z. Z. Li, K. Kadowaki, D. G. Hinks, Z. J. Xu, J. S. Wen, G. Gu, C. T. Lin, H. Claus, M. R. Norman, M. Randeria and J. C. Campuzano, Observation of a d-wave nodal liquid in highly underdoped $\text{Bi}_2\text{Sr}_2\text{CaCu}_2\text{O}_{8+\delta}$, *Nature Physics* **6**, 99103 (2010).
- [36] A. de la Torre, S. McKeown Walker, F. Y. Bruno, S. Riccò, Z. Wang, I. Gutierrez Lezama, G. Scheerer, G. Girit, D. Jaccard, C. Berthod, T. K. Kim, M. Hoesch, E. C. Hunter, R. S. Perry, A. Tamai, and F. Baumberger, Collapse of the Mott Gap and Emergence of a Nodal Liquid in Lightly Doped Sr_2IrO_4 , *Phys. Rev. Lett.* **115**, 176402 (2015).
- [37] Y. K. Kim, N. H. Sung, J. D. Denlinger and B. J. Kim, Observation of a d-wave gap in electron-doped Sr_2IrO_4 , *Nature Physics* **12**, 3741 (2016).